Canonical approach to finite density QCD with multiple precision computation

Ryutaro Fukuda,[1,2] Atsushi Nakamura,[3] and Shotaro Oka[4]

[1] *Department of Physics, The University of Tokyo, 7-3-1 Hongo, Bunkyo-ku, Tokyo 113-0033, Japan*
[2] *Institute für Theoretische Physik, ETH Zürich, CH-8093 Zürich, Switzerland*
[3] *Research Center for Nuclear Physics, Osaka University, Ibaraki 567-0047, Japan*
[4] *Department of Physics, Rikkyo University, 3-34-1 Nishi-Ikebukuro, Toshima-ku, Tokyo 171-8501, Japan*

We calculate the baryon chemical potential (μ_B) dependence of thermodynamic observables, i.e., pressure, baryon number density and susceptibility by lattice QCD using the canonical approach. We compare the results with those by the multi parameter reweighting (MPR) method; Both methods give very consistent values in the regions where errors of the MPR are under control. The canonical method gives reliable results over $\mu_B/T = 3$, with T being temperature. Multiple precision operations play an important roll in the evaluation of canonical partition functions.

PACS numbers: 12.38.Gc, 12.38.Mh, 21.65.Qr, 25.75.Nq, 05.10.-a, 02.90.+p

I. INTRODUCTION

Quantum Chromodynamics (QCD) is the fundamental theory describing the strong interaction. It is well known that QCD has the rich phase structure at finite temperature and density [1]. And yet, regions that we can access with the perturbation are limited. Currently, the most promising method to explore the phase diagram is lattice QCD simulation which is first principle calculation of QCD.

Although the lattice QCD simulations are very successful to analyze the phase diagram of a finite temperature system, at finite density they have a severe problem, so-called sign problem, and outcomes of the first-principle calculation can be available only at small chemical potential range. In finite temperature and density systems, lots of physically interesting targets such as the early universe, neutron stars, quark matters are waited to be explored. Therefore, it is quite desirable to explore methods for investigating finite density QCD systems from ab initio calculation; this is the one of the urgent subjects in particle physics and nuclear physics.

The canonical approach we study in this paper is a promising candidate for this purpose. In Ref.[2], the fugacity expansion by a method of the hopping parameter expansion was constructed as a winding number expansion, and the chiral condensate as well as the thermodynamic quantities is studied. More detailed analyses were performed in Ref.[3] in a wide range of the temperature and chemical potential regions, and an indication of the transition was first observed below T_c and finite baryon density. In this paper, we address two questions:

1. Does the lattice canonical approach produce consistent results with the MPR ?

2. In obtaining the canonical partition functions for large baryon number, what is a role of the multi precision calculations ?

Basic concept of the canonical approach in QCD

In N_f flavor QCD case with the degenerate quark masses, the grand canonical partition function at finite temperature T and finite quark chemical potential μ_q is given in the path integral formalism as follows.

$$Z_{GC}(T,\mu_q) = \int d[U]\{\det\Delta(\mu_q)\}^{N_f} e^{-S_{\rm g}}, \qquad (1)$$

where $\det\Delta(\mu_q)$ is the one flavor fermion determinant and $S_{\rm g}$ is the gauge action. Because the fermion determinant has the property

$$[\det\Delta(\mu_q)]^* = \det\Delta(-\mu_q^*), \qquad (2)$$

the Monte Carlo measure $\{\det\Delta(\mu_q)\}^{N_f} e^{-S_{\rm g}}$ becomes complex number at finite real chemical potential and the standard Monte Carlo method breaks down. Consequently, we cannot study finite density thermodynamics with standard grand canonical method. This difficulty is called sign problem.

A system described by the grand canonical partition function $Z_{GC}(T,\mu_q)$ is equivalent to a system described by the canonical partition function $Z_C(n,T)$ with fugacity $e^{\mu_q/T}$ in thermodynamic limit. The relation of two ensembles can be written as a fugacity expansion[4] using eigen vectors of number operator $\hat{N}\,|n\rangle = n\,|n\rangle$,

$$\begin{aligned} Z_{GC}(T,\mu_q) &= {\rm Tr}\; e^{-(\hat{H}-\mu_q\hat{N})/T} \\ &= \sum_{n=-\infty}^{\infty} \langle n|\, e^{-\hat{H}/T}\,|n\rangle\, e^{n\mu_q/T} \\ &\equiv \sum_{n=-\infty}^{\infty} Z_C(n,T)\; e^{n\mu_q/T}, \end{aligned} \qquad (3)$$

where $e^{\mu_q/T}$ is fugacity. If we have the canonical partition functions, $Z_C(n,T)$, for all net quark numbers n, we can construct the grand canonical partition function as a polynomial of fugacity with coefficients Z_C. From this

formula, one can obtain Lee-Yang zeros[5], which reflect the system's critical nature[6].

The canonical partition functions are constructed through the Fourier transformation of grand canonical partition function at pure imaginary chemical potential[7],

$$Z_C(n,T) = \frac{1}{2\pi}\int_0^{2\pi} d\left(\frac{\mu_I}{T}\right) Z_{GC}\left(\frac{i\mu_I}{T}\right) e^{-in\mu_I/T}, \quad (4)$$

where $\mu_I \in \mathbb{R}$. Eq.(2) tells us that the fermion determinant is real in the case of pure imaginary chemical potential. Monte Carlo simulations can then be performed and the canonical partition functions are obtained by Eq.(4). Eq.(4) also insists that the canonical partition fuctions are real number because the grand canonical partition function is even function (charge conjugation invariant) in terms of chemical potential. Considering this feature with Eq.(3), one can find that canonical partition functions are real and positive also in the context of canonical approach.

Once Z_C are available, we can construct the grand partition function by Eq.(3) at any *real* quark chemical potential. This is because the chemical potential dependence of the grand canonical partition function appears only through fugacity, $e^{\mu_q/T}$, which is the variable of the polynomial, and not in the coefficients, Z_C in Eq.(3); the effect of the chemical potential appears through the fugacity and the canonical partition function plays just a role of coefficients in the fugacity expansion of the grand canonical partition function.

II. FRAMEWORK

A. Winding number expansion of grand Partition function

In this work, we employ the RG-improved gauge action

$$S_{\rm g} = \frac{\beta}{6}\left[c_0 \sum_{n,\mu<\nu} W^{1\times1}_{\mu\nu}(n) + c_1 \sum_{n,\mu<\nu} W^{1\times2}_{\mu\nu}(n)\right] \quad (5)$$

with $c_1 = -0.331$ and $c_0 = 1 - 8c_1$, and the clover improved Wilson fermion action with the quark matrix

$$\begin{aligned}\Delta(n,m,\mu_q) =& \delta_{nm} - \kappa C_{SW}\delta_{nm}\sum_{\mu\le\nu}\sigma_{\mu\nu}F_{\mu\nu} \\ &- \kappa\sum_{i=1}^{3}\Big[(1-\gamma_i)\,U_i(n)\delta_{m,n+\hat{i}} \\ &\qquad + (1+\gamma_i)\,U_i^\dagger(m)\delta_{m,n-\hat{i}}\Big] \\ &- \kappa\Big[e^{+\mu_q a}(1-\gamma_4)U_4(n)\delta_{m,n+\hat{4}} \\ &\qquad + e^{-\mu_q a}(1+\gamma_4)U_4^\dagger(m)\delta_{m,n-\hat{4}}\Big] \\ &\equiv 1 - \kappa Q(\mu_q). \end{aligned} \quad (6)$$

Here n, m are space-time coordinates on a lattice, κ is hopping parameter and μ_q is the quark chemical potential which is introduced to the temporal part of link variables.

In order to obtain canonical partition functions, we need to compute the grand canonical partition functions at various pure imaginary chemical potential values in Fourier transformation Eq.(4).

We use the reweighting method to evaluate the grand canonical partition function,

$$\begin{aligned} Z_{GC}(i\mu_I) &= \int dU \left[\frac{\det\Delta(i\mu_I)}{\det\Delta(\mu_0)}\right]^{N_f} \{\det\Delta(\mu_0)\}^{N_f}\ e^{-S_g} \\ &= \left\langle\left[\frac{\det\Delta(i\mu_I)}{\det\Delta(\mu_0)}\right]^{N_f}\right\rangle_{\mu_0} Z_{GC}(\mu_0), \end{aligned} \quad (7)$$

where $\mu_0 = 0$ or pure imaginary values. We can then evaluate the canonical partition function as

$$\frac{Z_C(n,T)}{Z_C(0,T)} = \frac{1}{2\pi}\int_0^{2\pi} d\left(\frac{\mu_I}{T}\right) Z_{GC}(i\mu_I)\, e^{in\mu/T}. \quad (8)$$

We adopt, here, normalized canonical partition functions Eq.(8) in order to avoid the extra constant $Z_{GC}(\mu_0)$ in Eq.(7); this step does not affect the physical result. Now the evaluation of the grand canonical partition function is reduced to the calculation of ratios of fermion determinants in Eq.(7).

Performing the hopping parameter expansion in the logarithm, we write the fermion determinant as

$$\begin{aligned}\det\Delta(i\mu_I) &= \exp\Big[\mathrm{Tr}\log\{1-\kappa\Delta(i\mu_I)\}\Big] \\ &= \exp\left[-\mathrm{Tr}\sum_{j=1}^{\infty}\frac{\kappa^i}{j}Q^j(i\mu_I)\right]. \end{aligned} \quad (9)$$

The trace is taken over space-time, spinor and color. Here, we used the following identity for arbitrary matrix A:

$$\det A = e^{\log\det A} = e^{\mathrm{Tr}\log A}, \quad (10)$$

and log is expanded assuming κ is small (hopping parameter expansion).

The contribution of the trace in Eq.(9) comes from all closed loops on a lattice, and the chemical potential dependence comes from specific closed loops winding along positive and negative time directions. We can thus classify the trace of the hopping parameter expansion in Eq.(9) according to the winding number which is the number of net windings along the time direction. As a result, we can reach following expression with coefficients W_n and complex fugacity $e^{i\mu_I/T}$. Here n represents the winding number.

$$\det\Delta(i\mu_I) = \exp\left[\sum_{n=-\infty}^{\infty} W_n e^{in\mu_I/T}\right]. \quad (11)$$

We call this expression as 'winding number expansion'. The negative winding number appeared in Eq.(11) stands

for the winding along negative time direction. The coefficients W_n has no chemical potential dependence; the chemical potential dependence appears in the fugacity. Consequently, we have only to calculate W_n from given gauge configurations to obtain grand canonical partition functions at desired pure imaginary chemical potential.

B. Constraint on canonical partition function from symmetry of QCD

Roberge and Weiss pointed out that the QCD grand canonical partition at pure imaginary chemical potential has the following periodicity[8]

$$Z_{GC}\left(\frac{i\mu_I}{T}\right) = Z_{GC}\left(\frac{i\mu_I}{T} + \frac{2\pi ik}{3}\right), \tag{12}$$

where $k \in \mathbb{N}$. Using Eq.(12), we rewrite the grand canonical partition function as

$$Z_{GC}\left(\frac{i\mu_I}{T}\right) = \frac{1}{3}\sum_{k=0}^{2} Z_{GC}\left(\frac{i\mu_I}{T} + \frac{2\pi ik}{3}\right). \tag{13}$$

Then, we get the following relation,

$$Z_C(n,T) = \frac{1}{2\pi}\int_0^{2\pi} d\left(\frac{\mu_I}{T}\right) Z_{GC}\left(\frac{i\mu_I}{T}\right) e^{-in\mu_I/T} \times \left[\frac{1 + e^{i\frac{2\pi}{3}n} + e^{i\frac{4\pi}{3}n}}{3}\right]. \tag{14}$$

We obtain the following important constraint on the canonical partition functions,

$$Z_C(n \neq 3k) = 0. \tag{15}$$

Note that this holds both in the confinement and the deconfinement phases.

Now the grand partition function can be written as

$$Z_{GC}(T,\mu_B) = \sum_{B=-\infty}^{\infty} Z_C(B,T)e^{B\mu_B/T}, \tag{16}$$

where $B \in \mathbb{N}$. Because this quantum number B can be interpreted as net baryon number, μ_B can be regarded as baryon chemical potential which is related to quark chemical potential as $\mu_B = 3\mu_q$.

C. Thermodynamic observables

In a homogeneous system, the dimensionless equation of state at (μ_B, T) is given by

$$\frac{p(\mu_B,T)}{T^4} = \frac{1}{V_s T^3}\log Z_{GC}(\mu_B,T) = \left(\frac{N_t}{N_s}\right)^3 \log Z_{GC}(\mu_B,T), \tag{17}$$

where $N_s = N_x = N_y = N_z$ and $T^{-1} = N_t a$ with a lattice spacing a. The deviation of the pressure from $\mu_B = 0$ is given by

$$\frac{\Delta p(\mu_B,T)}{T^4} = \frac{p(\mu_B,T)}{T^4} - \frac{p(0,T)}{T^4} = \left(\frac{N_t}{N_s}\right)^3 \log\left(\frac{Z_{GC}(\mu_B,T)}{Z_{GC}(0,T)}\right). \tag{18}$$

The dimensionless baryon number density n_B/T^3 and susceptibility χ/T^2 are

$$\frac{n_B(\mu_B,T)}{T^3} = \frac{\partial}{\partial(\mu_B/T)}\frac{p(\mu_B,T)}{T^4}, \tag{19}$$

$$\frac{\chi(\mu_B,T)}{T^2} = \frac{\partial^2}{\partial(\mu_B/T)^2}\frac{p(\mu_B,T)}{T^4}. \tag{20}$$

III. NUMERICAL RESULTS

A. Lattice set up

We adopt 2-flavor clover improved Wilson fermion action with $C_{\rm SW} = (1 - 0.8412/\beta)^{-3/4}$ evaluated by one-loop perturbation theory and RG-improved gauge action. All simulations were performed on $N_x \times N_y \times N_z \times N_t = 8 \times 8 \times 8 \times 4$ lattice. We considered $\beta = 2.00$, 1.95, 1.90, 1.85, 1.80, 1.70 which correspond to $T/T_c = 1.35(7)$, 1.20(6), 1.08(5), 0.99(5), 0.93(5), 0.84(4)[9]. The values of hopping parameter κ was determined for each β by following the line of the consistent physics in case of $m_\pi/m_\rho = 0.8$ in Ref.[9].

We generated gauge configurations at $\mu_0 = 0$ with the hybrid Monte Carlo (HMC) method. The step size $d\tau$ and number of steps N_τ of HMC were set to $\delta\tau = 0.02$, $N_\tau = 50$ so that the simulation time was $d\tau \times N_\tau = 1$. After the first 2000 trajectories for thermalization, we adopted 400 configurations every 200 trajectories for each parameter set.

B. Instability of Fourier transformation in canonical approach and its solution

Before proceeding to our numerical results, we refer to the instability of Fourier transformation in canonical approach and then discuss our strategy to avoid it in this subsection.

Since the fugacity expansion of grand canonical partition function, Eq.(3), converges at real baryon chemical potential, the canonical partition function Z_n must become smaller when the net baryon number $|n|$ becomes large. This means that we have to deal with quite small values as the results of Fourier transformation. This step is quite difficult in the point of view of numerical calculation because the Fourier transformation is an oscillatory integral.

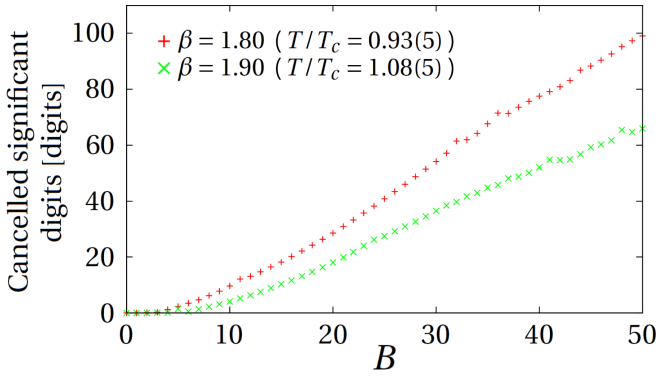

FIG. 1. (Color online) Cancelled significant digits in calculations of DFT at over T_c (upper red points) and below T_c (lower green points).

1. *Instability of Fourier transformation*

In numerical calculation, Fourier transformation Eq.(4) is computed by discrete Fourier transformation (DFT) as

$$Z_C(n,T) = \frac{1}{N}\sum_{k=0}^{N-1} Z_{GC}\left(i\frac{\mu_I}{T} = i\frac{2\pi k}{N}\right) e^{i\frac{2\pi k}{N}n}, \quad (21)$$

where N is the interval number of DFT. Because DFT is just a discretized version of Fourier transformation in continuum theory, the instability of DFT in canonical approach is simply caused by the numerical errors. They are classified into rounding error, truncation error, cancellation of significant digits and loss of trailing digits. The instability of DFT does not come from truncation error since DFT is not infinite series. Accordingly, it is quite natural to consider that the instability originates from cancellation of significant digits or loss of trailing digits or both of them. In this work, we actually monitored the behavior of all variables in our DFT program in order to study the effect of these two errors. As the result, we found that cancellation of significant digits is not negligible in DFT program. Fig.1 represents cancelled digits in DFT. For example, 80 digits are cancelled in case of $\beta = 1.80$, $B = n/3 = 40$. We also found that the appearance of the cancellation does not depend on temperature of a system.

2. *Solution of instability - multiple length precision calculation*

Cancellation of significant digits arises from the following types of calculation,

$$\begin{array}{lll} 1.234567 - 1.234566 & = & 0.000001 \\ \text{(7 significant digits)} & & \text{(1 significant digit)} \end{array} \quad (22)$$

In this case, six significant digits are lost.

In order to reduce the effect of this cancellation, we should increase significant digits as a solution. Let us consider the next calculation with 22 significant digits.

$$\begin{array}{l} 1.234567444444444444444 - 1.234566111111111111111 \\ \text{(22 significant digits)} \\ \qquad = \ 0.000001333333333333333 \\ \qquad\quad \text{(16 significant digits)} \end{array} \quad (23)$$

Although six significant digits are definitely lost in this calculation, 16 significant digits survive in the final result.

Summarizing above, the precision of the result can be kept by increasing significant digits of variables in this way. Fig.2 represents the cancelled digits in the calculation of $Z_C(B,T)$ with 16, 32, 48, 64 precision calculation. According to this figure, for evaluating $Z_C(B,T)$ to larger n, it is essential to increase significant digits of variables.

C. Thermodynamic observables at finite real baryon chemical potential

1. *Calculation procedure*

First, we computed coefficients of winding number expansion W_n up to $n = 120$ with 400 configurations in all temperature cases. We used 64 (above T_c) and 128 (below T_c) noise vectors to calculate the trace in the fermion determinant Eq.(9). Then, we evaluated the grand canonical partition functions at various pure imaginary chemical potentials using the winding number expansion with W_n. After that, we evaluated the canonical partition function through Fourier transformation and thermodynamic observables. We adopted multiple length precision calculation[10] with 400 significant digits in order to keep the sufficient precision except for the calculation of gauge configurations and W_n. Gauge configurations and W_n were computed with double precision, i.e., around 16 significant digits.

Note that canonical partition functions are complex number in numerical calculations because of numerical errors. Therefore, we adopt the only real part of the canonical partiton function. If the real part of the canonical partition function is negative at some baryon number n_B fo the first time, we adopt the result up to $n_B - 1$ as canonical partiton functions.

2. *Estimation of truncation error in fugacity expansion*

In numerical calculation, we have to deal with the fugacity expansion of the grand canonical partition function as the finite series

$$Z_{GC}(T,\mu_B) = \sum_{B=-N_{\max}}^{N_{\max}} Z_C(B,T)e^{B\mu_B/T}. \quad (24)$$

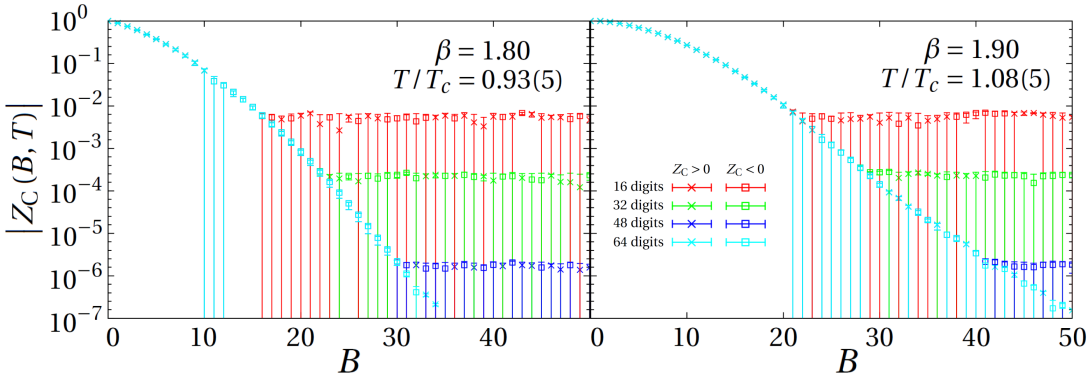

FIG. 2. (Color online) Relation between behavior of $Z_C(B,T)$ and precision of variables, at over T_c (left panel) and below T_c (right panel). Both panels are plotted with some precision at 16 digits (double precision, uper red points), 32 digits (second green points), 48 digits (third blue points), and 64 digits (lowest cyan points).

Therefore, we have to judge the baryon chemical potential region where results are free from the truncation error. There may be several possible ways to analyze the effect of the truncation error; In this work, we use the following analysis.

First, we evaluate the expectation values of thermodynamic observables $\langle O(\mu_B)\rangle_{N_{\max}}$ with Eq.(24). Next, we calculate the expectation values $\langle O(\mu_B)\rangle_{N_{\max-1}}$ by subtracting one from $N_{\max}$ in Eq.(24). After that, we evaluate the relative error $R_{\rm ob}(\mu_B)$ from these two expectation values; and in this work we judge that the expectation value is reliable if the relative error is less than 10^{-3},

$$R_{\rm ob}(\mu_B) \equiv 1 - \frac{\langle O\rangle_{N_{\max-1}}}{\langle O\rangle_{N_{\max}}} < 10^{-3}. \qquad (25)$$

In this way, we can ensure that expectation values of thermodynamic observables in the baryon chemical potential region determined by above analysis have two significant digits at least against the truncation error.

3. *Thermodynamic observables*

Using the error estimation described in the previous subsection, we analyze the chemical potential dependence of thermodynamic observables and study the validity of canonical approach. First, we examine the pressure. Fig.3 shows that the results of pressure above T_c do not suffer from large error up to around $\mu_B/T = 5$, and the results below T_c are under control up to $\mu_B/T = 3.5-4$. On the other hand, the result just below T_c case is reliable only up to around $\mu_B/T = 3$. This may be because we make configurations at $\mu_0 = 0$ and the configurations are suffered from the fluctuation caused by the phase transition at zero density. We may get clearer signals if we generate configurations at pure imaginary chemical potential because T_c at pure imaginary chemical potential is higher than T_c at zero chemical potential.

In Fig.4, we see that pressure calculated by canonical approach are consistent with results by MPR.

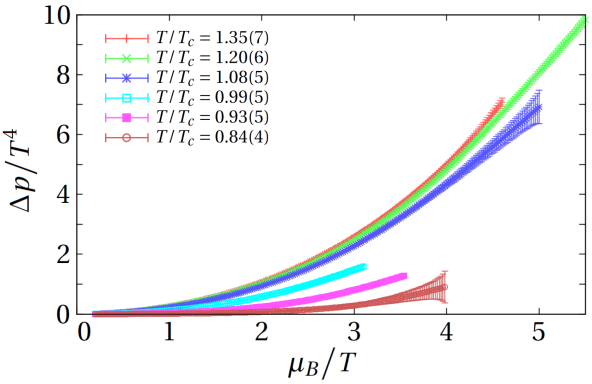

FIG. 3. (Color online) Chemical potential dependence of pressure. Red, green, blue, cyan, magenta and brown points are the results at $T/T_c = 1.35, 1.20, 1.08, 0.99, 0.93$ and 0.83. Upper bound of baryon chemical potential is determined by Eq.(25).

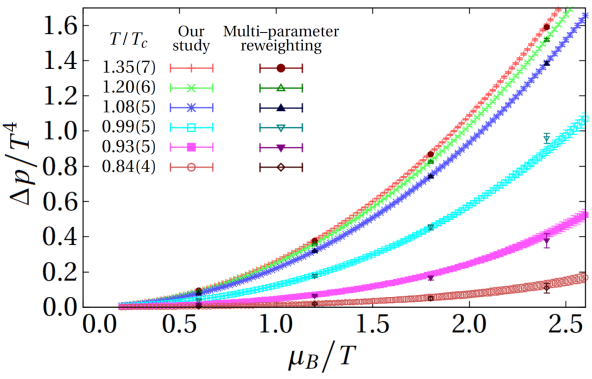

FIG. 4. (Color online) Comparison of pressure calculated by canonical approach and multi parameter reweighting method. Basically, color of data are same as Fig.3. Extra color: dark–red, dark–green, dark–blue, dark–cyan, dark–magenta and dark–brown points are the results at $T/T_c = 1.35, 1.20, 1.08, 0.99, 0.93$ and 0.83 calculated by multi–parameter reweighting method.

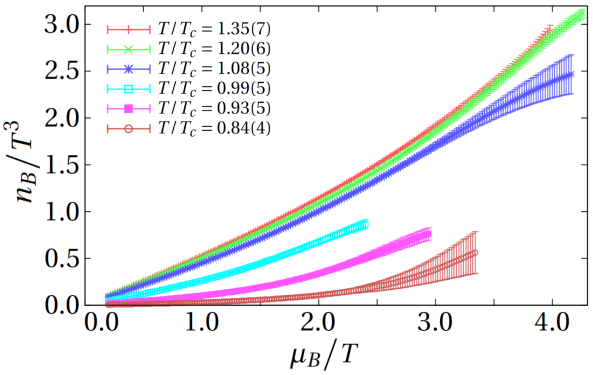

FIG. 5. (Color online) Chemical potential dependence of baryon number density. Color of data are same as Fig.3. Upper bound of baryon chemical potential is determined by Eq.(25).

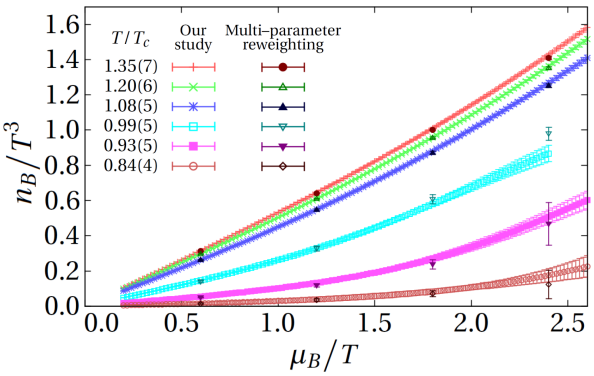

FIG. 6. (Color online) Comparison of the baryon number density calculated by canonical approach and multi parameter reweighting method. Color of data are same as Fig.4.

Next, we consider the expectation value of the baryon number density. In Fig.5, we find that the results are reliable up to around $\mu_B/T = 4$ ($\mu_B/T = 3 - 3.5$) above T_c (below T_c). While, the reliable baryon chemical potential range of the result just below T_c is limited up to $\mu_B/T = 2.4$. This may be caused by the same reason in the analysis of the pressure.

Fig.6 tells us that the canonical approach is consistent with MPR method also in the baryon number density case. Moreover, we observe that the gradient of the baryon number density, n_B, as a function of baryon chemical potential becomes smaller as the temperature decreases. In zero temperature case, n_B is expected to be zero up to $\mu_B/T = m_B/T$, where m_B is the lightest baryon mass of the system and it becomes a finite value at this point. Indeed, the data at $T/T_c = 0.84$ shows such a feature.

Finally, we investigate the susceptibility. Fig.7 shows that the results above T_c is reliable up to around $\mu_B/T = 3.5$, while the results below T_c is reliable up to $T_c = 2.4 - 2.9$. From Fig.8, we find that canonical approach is very consistent with MPR method also in the susceptibility.

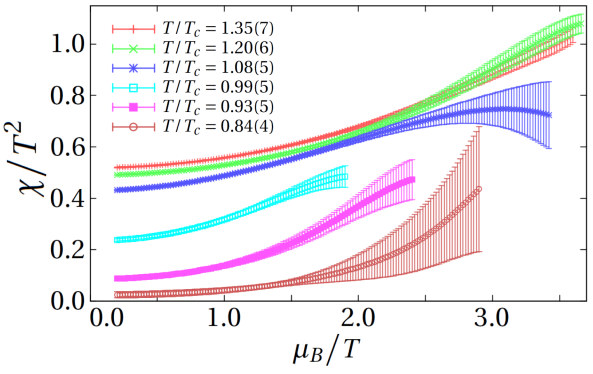

FIG. 7. (Color online) Chemical potential dependence of susceptibility. Color of data are same as Fig.3. Upper bound of baryon chemical potential is determined by Eq.(25).

The susceptibility as a function of the μ_B/T does not show a clear peak; we do not see yet the signal of the phase transition between confined phase and deconfined phase.

IV. SUMMARY AND OUTLOOK

In this paper, we find that the canonical approach is consistent with MPR method. Moreover, the canonical approach provides reliable results beyond $\mu_B/T = 3$ in almost all observables. This is very encouraging for the first principle calculation of finite density QCD, because other methods such as MPR method, Taylor expansion method and imaginary chemical potential method give reliable information practically only up to $\mu_B/T = 3$. The multiple precision calculation greatly contributes this conclusion.

The canonical approach has been investigated several times [7, 11–15] ; We brush up the method here and find that it is a useful and promising method. But, we have to improve our method further to obtain results in more realistic condition, i.e., lighter quark mass, large volume, finer lattice spacing and larger density. Although the hopping parameter expansion gave very interesting results as we saw in this paper, the next step is to calculate the fermion determinant without this approximation; we have learned in this paper that the key point is to calculate the determinant at imaginary chemical potential values that are Fourier transformed with high accuracy in Eq.(4). This requires more computational resource than the work reported here, but within scope of the next generation high performance era.

ACKNOWLEDGMENTS

This work is done for Zn Collaboration: We would like to thank the members of Zn collaboration, S. Sakai, A. Suzuki and Y. Taniguchi for their powerful support. We appreciate useful discussions with K. Fukushima and

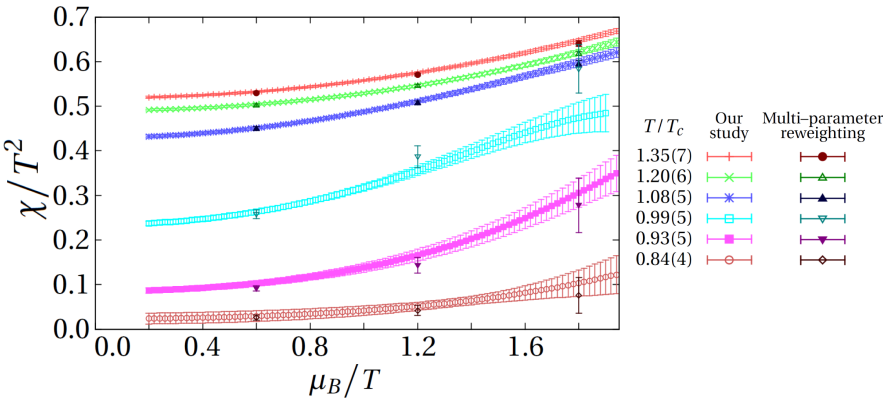

FIG. 8. (Color online) Comparison of susceptibility calculated by canonical approach and multi parameter reweighting method. Color of data are same as Fig.4.

Ph. de Forcrand. R. F. thanks the Yukawa Institute for Theoretical Physics, Kyoto University. Discussions during the YITP workshop YITP-T-14-03 on "Hadrons and Hadron Interactions in QCD" were useful to complete this work. R. F. also would like to thank ETH for its warm hospitality. S. O. acknowledges T. Eguchi for valuable discussions and encouragement. This work is supported in part by Grants-in-Aid of the Ministry of Education (Nos. 15H03663, 26610072). The calculations were done with SX-9 and SX-ACE at RCNP (Osaka), SR16000 at the Yukawa Institute for Theoretical Physics (Kyoto).

[1] K. Fukushima and T. Hatsuda, Rept. Prog. Phys. **74**, 014001 (2011);
[2] A. Nakamura, S. Oka and Y. Taniguchi, arXiv:1504.04096 [hep-lat].
[3] A. Nakamura, S. Oka and Y. Taniguchi, arXiv:1504.04471.
[4] K. Nagata and A. Nakamura JHEP, 1204, 092 (2012). (arXiv:1201.2765)
[5] Atsushi Nakamura and Keitaro Nagata, arXiv:1305.0760
[6] C. N. Yang and T. D. Lee, Phys. Rev. **87**, 404 (1952), T. D. Lee and C. N. Yang, Phys. Rev. **87** (1952) 410.
[7] A. Hasenfratz and D. Toussaint, Nucl. Phys B371 (1992) 539.
[8] A. Roberge and N. Weiss, Nucl. Phys. B275(1986) 734.
[9] S. Ejiri, Y. Maezawa, N. Ukita, S. Aoki, T. Hatsuda, N. Ishii, K. Kanaya, and T. Umeda (WHOT-QCD Collaboration), Phys. Rev. D 82, 014508 (2010).
[10] D. M. Smith, `http://myweb.lmu.edu/dmsmith/FMLIB.html`
[11] P. de Forcrand and S. Kratochvila, Nucl. Phys. Proc. Suppl. **153**, 62 (2006) [hep-lat/0602024].
[12] A. Li, A. Alexandru and K. F. Liu, Phys. Rev. D **84**, 071503 (2011) [arXiv:1103.3045 [hep-ph]].
[13] A. Alexandru, M. Faber, I. Horvath and K. F. Liu, Phys. Rev. D **72**, 114513 (2005) [hep-lat/0507020].
[14] X. f. Meng, A. Li, A. Alexandru and K. F. Liu, PoS LATTICE **2008**, 032 (2008) [arXiv:0811.2112 [hep-lat]].
[15] A. Li, A. Alexandru, K. F. Liu and X. Meng, Phys. Rev. D **82**, 054502 (2010) [arXiv:1005.4158 [hep-lat]].